Salinity Contribution to Regional Sea Level Trends in the Tropical Southwestern Pacific Ocean Over 2014–2023

William Llovel, Antoine Hochet

Geophysical Research Letters

RESEARCH LETTER
10.1029/2025GL116115

Salinity Contribution to Regional Sea Level Trends in the Tropical Southwestern Pacific Ocean Over 2014–2023

William Llovel[1] **and Antoine Hochet**[1]

[1]University Brest, CNRS, Ifremer, IRD, Laboratoire d'Océanographie Physique et Spatiale (LOPS), IUEM, Plouzané, France

Key Points:

- Valuable contribution of Argo data to the interpretation of satellite altimetry data for the study of contemporary regional sea level trends
- Upper ocean salinity increase contributes to regional sea level trends
- Importance of local precipitation and remote wave propagation to explain the increase in salinity recorded by Argo floats

Correspondence to:

W. Llovel,
william.llovel@ifremer.fr

Citation:

Llovel, W., & Hochet, A. (2025). Salinity contribution to regional sea level trends in the Tropical Southwestern Pacific Ocean over 2014–2023. *Geophysical Research Letters*, *52*, e2025GL116115. https://doi.org/10.1029/2025GL116115

Received 21 MAR 2025
Accepted 22 AUG 2025

Author Contributions:

Conceptualization: William Llovel, Antoine Hochet
Data curation: William Llovel
Funding acquisition: William Llovel
Investigation: William Llovel
Methodology: William Llovel, Antoine Hochet
Software: William Llovel
Writing – original draft: William Llovel
Writing – review & editing: Antoine Hochet

Abstract Steric sea-level has been identified as the main driver of regional sea-level trends. Altimetry-based spatial patterns vary as a function of space and time. Thermosteric (temperature-related) sea-level trends have generally been found to be more important than the halosteric (salinity-related) trends. Using satellite altimetry data together with an Argo-based gridded product, we find a negative trend in halosteric sea-level in the Tropical Southwestern Pacific Ocean over 2014–2023, which attenuates thermosteric sea-level trends during this period. This striking negative halosteric trend is associated with salinization of the upper 400 m, which is related to both salinity anomalies on isopycnal surfaces and to the vertical movement of isopycnals. This salinization can be explained by a precipitation deficit and by a remote contribution from wind-driven wave propagation. Our results highlight the importance of salinity changes when interpreting satellite altimetry data.

Plain Language Summary Investigating regional sea level change is important as ∼10% of the world's population lives at an altitude below 10 m above sea level. Based on satellite altimetry data and upper ocean temperature and salinity changes inferred from an Argo-based gridded product, we investigate the regional sea level trends in the Tropical Southwestern Pacific Ocean, where we find a strong compensation between temperature-induced and salinity-induced sea level trends. We focus on the salinity-induced sea level decline over 2014–2023 and find that this decline is associated with ocean salinization in the upper 400 m, which may be due to the precipitation deficit and remote wave propagation induced by surface wind stress forcing. Our study demonstrates the complementarity between remote sensing data based on satellite altimetry and in situ measurements of temperature and salinity profiles recorded by autonomous Argo platforms.

1. Introduction

Sea level rise is a major consequence of global warming. Global mean sea level rise has been routinely measured with unprecedented accuracy by satellite altimetry since the launch of TOPEX/Poseidon in August 1992 (Cazenave et al., 2019). Its successors (Jason-1/-2/-3 and Sentinel-6 MF) provide the continuity of the time series, and now +32 years of data allow these changes to be studied (International Altimetry Team, 2021). This global mean sea level rise is due to global ocean warming (known as thermosteric sea level) and barystatic sea level component (i.e., global ocean mass change induced by continental ice melting; Gregory et al., 2019).

Satellite altimetry data reveal large regional variability in sea level trends, with some regions experiencing decadal rises two times greater than the global mean trend (Cazenave & Moreira, 2022; Llovel et al., 2018). At the regional scale, sea level change is driven by changes in regional mass and local temperature and salinity, which affect the properties of the water mass (Stammer et al., 2013; Tajouri et al., 2024). These regional changes are driven by heat/fresh water and momentum air-sea fluxes (Hochet et al., 2023, 2024; Stammer et al., 2013). A better understanding of the physical processes involved in the observed regional sea level trends in recent years and decades is essential for the correct interpretation of satellite altimetry observations and for assessing the reliability of coupled climate models used to predict future sea level rise.

In the equatorial Pacific, regional sea level rise has been two times greater than the global mean trend since 1993 (Cazenave & Moreira, 2022). The western tropical Pacific contains many of the world's low-lying and densely populated coastal regions. This region is commonly considered to be one of the most vulnerable to future sea-level rise (Nicholls & Cazenave, 2010). Indeed, this region is home to volcanic archipelagos of low-lying islands and atolls, where solid earth signals (e.g., vertical land movements due to tectonics and volcanism; subsidence due to groundwater and/or oil extraction; urbanization) can exacerbate climate-induced sea-level rise (Nicholls et al., 2021).

While the contribution of temperature to regional sea level has been studied for years, the contribution of salinity change to sea level has been less studied due to salinity's negligible impact on global mean sea level (Llovel et al., 2019; Munk, 2003) and the lack of historical salinity measurements. With the development of the international Argo program, salinity profiles have been collected from autonomous platforms for the upper 2,000 dbar since the beginning of the 2000s (Roemmich et al., 2019; Zilberman et al., 2023). Based on Argo products, it has been shown that the contribution of salinity accounts for ∼60% of the regional sea level trend inferred from satellite altimetry measurements in the southeast Indian Ocean (Llovel & Lee, 2015) over 2005–2013. This study highlights the non-negligible contribution of salinity to regional sea level trends on a 9-year period. The Argo data record has now reached more than 2 decades, providing us with the opportunity to assess the decadal changes in temperature and salinity contributions to regional sea level trends inferred from satellite altimetry data for the last decade (i.e., 2014–2023). This is the purpose of the current paper.

The paper is organized as follows. Section 2 describes the data and the methods used in this study. In Section 3, we presents our results on the upper ocean salinity increase to regional sea level trends in the Tropical Southwestern Pacific Ocean including an investigation into the local and remote atmospheric forcing mechanisms. Finally, Section 4 summarizes ours findings, addresses their broader implications and outlines future research.

2. Data and Methods

2.1. Satellite Altimetry Data

We consider the satellite altimetry data provided by the Copernicus Marine Service (https://data.marine.copernicus.eu/product/SEALEVEL_GLO_PHY_L4_MY_008_047/description). This product provides the gridded sea level anomalies computed with respect to the 1993–2012 time average. Along-track satellite altimetry data from the reference missions (TOPEX/Poseidon, Jason-1/-2-3 and Sentinel-6 MF) have been interpolated to a regular grid using an optimal interpolation method over the period 1993–2023. Geophysical corrections (ionospheric, wet and dry troposphere, tides, sea state, etc.) have been applied to the data set (Ablain et al., 2019). The product is global (including the polar regions) with a spatial grid of 0.125° × 0.125°. Monthly mean data have been calculated based on daily mean estimates.

2.2. Temperature and Salinity Gridded Data

We consider a gridded temperature (T) and salinity (S) product provided by the Scripps Institute of Oceanography (SIO, updated from Roemmich and Gilson (2009)) based on Argo T/S profiles. This product has a spatial resolution of 1° × 1° from 64.5°S to 79.5°N and from 2.5 to 1,975 dbar. The T/S profiles have undergone several quality controls (Wong et al., 2020). The choice of the SIO product was motivated by the fact that the product rejects the near real time Argo floats that experience rapid salinity drifts (Liu et al., 2024; Ponte et al., 2021). As a significant fraction of near real-time Argo floats exhibit this salinity drift, the inclusion of such profiles has been shown to affect the non closure of the global mean sea level budget after 2016 (Barnoud et al., 2021; Llovel et al., 2023). This non-closure has been attributed, in part, to unrealistic halosteric behavior immediately after 2016. Here, we compute the steric, thermosteric, and halosteric sea level change (for the upper 2,000 m) on a monthly mean basis over January 2014–December 2023 using the TEOS10 equation of state for density (McDougall & Barker, 2011). We first convert T/S into conservative temperature and absolute salinity at each standard level. We then integrate in situ density anomalies (defined as differences between the density and a reference density at 0°C and 35.16504 g/kg) down to 1,975 dbar (for more details, see Llovel et al. (2013)).

2.3. Heave and Spice Decomposition

An isopycnal decomposition of salinity anomalies is performed to investigate the origin of salinity anomalies which can be associated with isopycnal motions (S'_{Heave}) and/or salinity anomalies on potential density surfaces (S'_{Spice}, Bindoff & Mcdougall, 1994). For this purpose, the SIO salinity grid data were interpolated in density space from 1,019 to 1,038 kg/m^3 (relative to the surface) with a density resolution of 0.1 kg/m^3. Mean salinity anomalies at fixed density correspond to the spice component, while pressure anomalies at fixed density surfaces multiplied by the vertical salinity gradient correspond to the heave component. Such an approach has been used to study the variability of ocean heat content in the North Atlantic (Häkkinen et al., 2015) or the variability of deep water masses in the Irminger Sea (Desbruyeres et al., 2022). We interpret the spice component as the advection of salinity anomalies within isopycnal surfaces, while the heave component is interpreted as dynamical changes

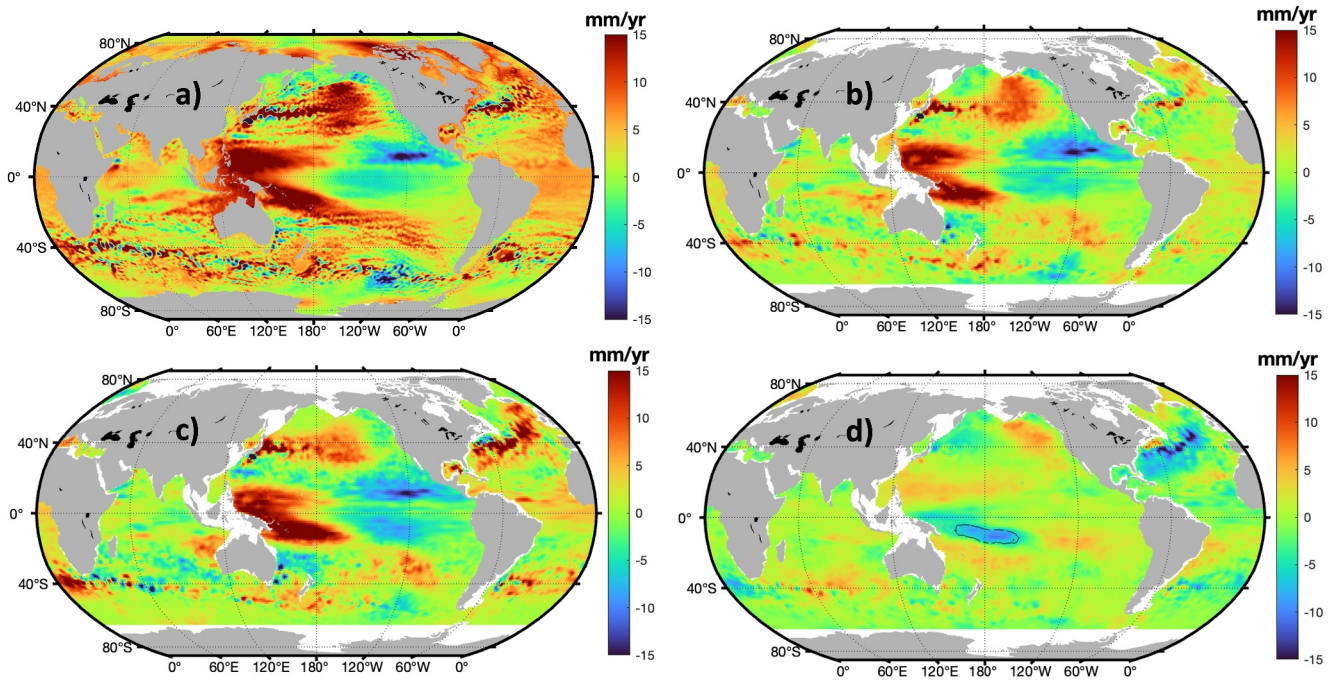

Figure 1. Sea level trend maps over 2014–2023 for (a) satellite altimetry data, (b) Argo-based steric component, (c) Argo-based thermosteric component, and (d) Argo-based halosteric component. Time series have been corrected for annual signal and are referenced to the time mean computed over 2014–2023.

induced by wind-driven Ekman pumping or wave propagation (local and/or remote contribution, respectively; Häkkinen et al., 2016; Huang et al., 2024; Volkov et al., 2017).

2.4. Surface Forcing Products

To complement the spice and heave decomposition of salinity anomalies, we analyze air-sea freshwater flux (precipitation minus evaporation, hereafter referred to as P − E) and Ekman pumping from the ERA5 data set (Hersbach et al., 2020) to assess both local and remote atmospheric forcing contributions. ERA5 is an atmospheric reanalysis that assimilates model data with observations into a globally complete and consistent framework. We consider the monthly mean estimates for P − E for the air-sea freshwater flux and the 10 m wind (U and V) to assess first the wind stress and then the Ekman pumping on a global grid with a spatial resolution of 0.25° × 0.25°. To assess the robustness of the precipitation fields, we also analyze the Global Precipitation Climatology Project product (GPCP, v2.3; Huffman et al., 2009), a 2.5° resolution global gridded data set merging satellite data and precipitation gauge measurements from 1979 onward.

2.5. Data Processing

All data sets described previously are analyzed over the period January 2014–December 2023, unless otherwise stated. As this study investigates decadal sea level change over 2014–2023, the monthly mean climatology is removed from the time series at each location for each data set. The climatology has been defined as the monthly mean for each calendar month computed over January 2014–December 2023.

3. Results

3.1. Sea Level Trends

Figure 1a shows the regional sea level trends inferred from satellite altimetry data over 2014–2023, that confirms large regional variability in sea level trends (Cazenave & Moreira, 2022; Llovel et al., 2018). Larger values are found in the Pacific Ocean: >15 mm/yr, in the western part, and negative decadal sea level trends in the eastern part. Figure 1b shows the map of regional steric sea level trends calculated for the period 2014–2023. The spatial patterns of steric sea level trends are in good agreement with those observed by satellite altimetry, especially in the

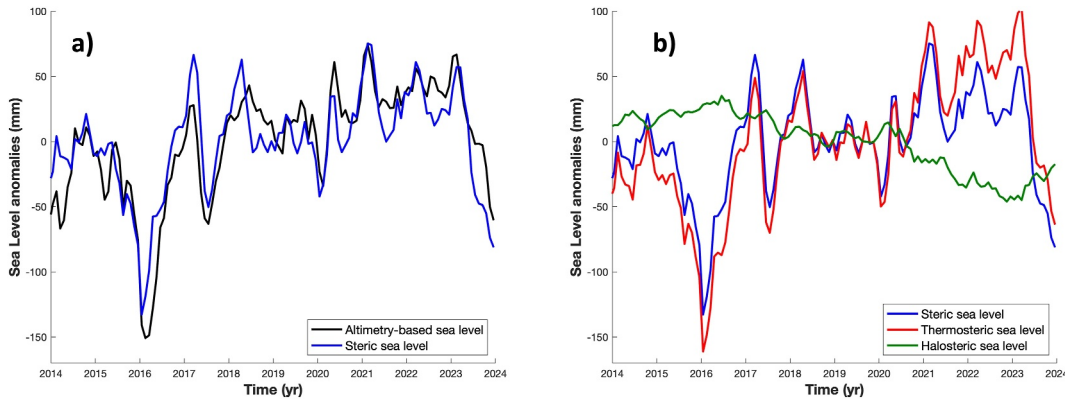

Figure 2. (a) Regionally averaged sea level and steric sea level (black and blue curves, respectively) and (b) regionally averaged thermo/halo/steric sea level times series (red, green, and blue curves, respectively).

Pacific Ocean (tropical and extra-tropical regions), confirming the steric origin of these patterns. However, we notice some differences between altimetry-based and Argo-based regional sea level trends that could be attributed to regional ocean mass changes and deep ocean steric sea level changes below 1,975 dbar (Johnson et al., 2020; Lele & Purkey, 2024; Llovel et al., 2014).

Figures 1c and 1d display the maps of thermosteric (temperature contribution) and halosteric (salinity contribution) sea level trends, respectively. Regional patterns of thermosteric sea level trends (Figure 1c) are comparable to those of steric sea level trends (Figure 1b) confirming that temperature change is the overall dominant contribution to regional sea level trends (Stammer et al., 2013). Halosteric sea level trends (Figure 1d) are over much of the world ocean smaller in amplitude. However, we find negative halosteric sea level trends (larger than −5 mm/yr) in the Tropical Southwestern Pacific Ocean (hereafter TSWPO). This halosteric sea level decrease is associated with an increase of salinity. This result is puzzling as this region has experienced a long term halosteric sea level rise (i.e., freshening) over 1950–2008 according to historical in situ data and climate models (Durack et al., 2014). Therefore, further investigations into the impact of this salinity increase on regional sea level trends is required.

3.2. Sea Level Change in the TSWPO

To better understand the role of salinity changes in regional sea level trends in the TSWPO, we defined an area where halosteric sea level trends are less than −4 mm/yr. The contour mask is shown by the black solid line in Figure 1d.

Figure 2a shows the mean sea level change (black line) and the steric sea level change (blue line) within the aforementioned masked region. Both curves depict large interannual variability around positive linear trends of 8.71 ± 2.31 mm/yr and 4.12 ± 2.33 mm/yr (2-sigma uncertainty), respectively. In this region, the satellite-based estimated linear trend is at 50% explained by the steric sea level trend contribution. Besides large uncertainties, the remaining 50% might come from the regional mass contribution and/or the deep ocean steric sea level (below 1,975 dbar, Lele & Purkey, 2024). The standard deviation of the detrended altimetry-based mean sea level is 36.5 mm, while the standard deviation of the detrended Argo-based steric sea level is 36.7 mm, confirming that the sea level internannual variability is of steric origin.

This regionally averaged steric sea level trend results from a compensation between the temperature (red curve) and salinity contributions (green curve, Figure 2 right panel) that account respectively for 10.91 ± 2.64 mm/yr and −6.79 ± 0.64 mm/yr of steric sea level trends. Therefore, the halosteric sea level trend in this specific region is large and reduces the effect of thermosteric sea level rise. The standard deviation of the detrended thermosteric sea level time series amounts of 41.6 mm whereas the halosteric standard deviation contribution is 10.2 mm. Thus, the steric sea level interannual variability in the TSWPO is mainly explained by temperature changes, while the salinity increase plays an important role in offsetting the thermosteric sea level rise. The question that naturally arises is: how is the increase in salinity vertically distributed in the TSWPO?

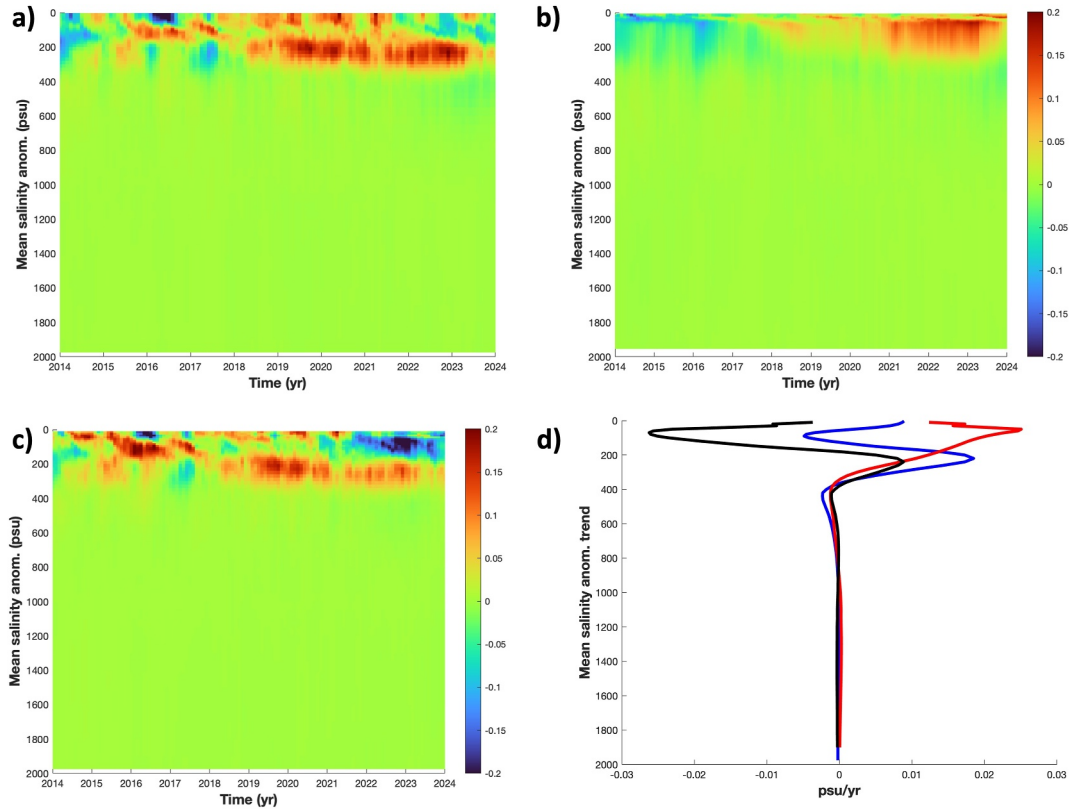

Figure 3. (a) Regionally averaged salinity anomalies as a function of depth in the Tropical Southwestern Pacific Ocean (TSWPO) ocean over 2014–2023; (b) spice and (c) heave contribution to the salinity anomalies as a function of depth. (d) Salinity trends (blue curve), heave and spice components (black and red curves) as a function of depth in the TSWPO over 2014–2023.

3.3. Salinity Change in the TSWPO

Figure 3a presents the regionally averaged salinity anomalies as a function of depth for the TSWPO. The maximum of salinity change is located at nearly 300 m with an intensification (up to 0.2 psu) starting in 2018. Figures 3b and 3c show the S'_{Spice} and S'_{Heave} contributions in the TSWPO over 2014–2023. We find that the S'_{Spice} component increases for the upper 300 m depth, reaching values of 0.2 psu by 2023. Figure 3c shows the S'_{Heave} highlighting similar patterns to the S' change in the TSWPO. Figure 3d displays the mean salinity trends (blue curve) as a function of depth. We find a freshening of around −0.005 psu/yr at 100 m and salinifications near the surface (0.01 psu/yr) and around 300 m depth (0.02 psu/yr). The black and red curves show the heave and spice salinity trends, respectively. The freshening observed at 100 m is due to the heave component being largely offset by the spice contribution. The increase in salinity at the surface is mainly driven by the spice component, whereas at a depth of around 300 m, the salinity increase results from both components, each accounting for 50%. Therefore, we conclude that the regionally averaged salinity anomalies for this region are located within the upper 400 m and are driven by both the heave and spice components.

3.4. Local Versus Remote Atmospheric Forcing

As both spice and heave changes are at play in these salinity changes, it suggests that local (P − E or Ekman pumping) and/or remote wind-driven (wave propagation) processes may be responsible for the regional halosteric sea level decrease. This raises the question of the origin of such upper ocean salinization in the TSWPO. Here, we investigate the increase in salinity, which can be associated with changes in ocean-air freshwater fluxes (P − E) and/or local Ekman pumping. The direct contribution from river runoff can be neglected as there is no major river in the TSWPO. We adopt the convention that a negative (positive) sign represents downward (upward) Ekman pumping and ocean freshwater loss (gain) in P − E.

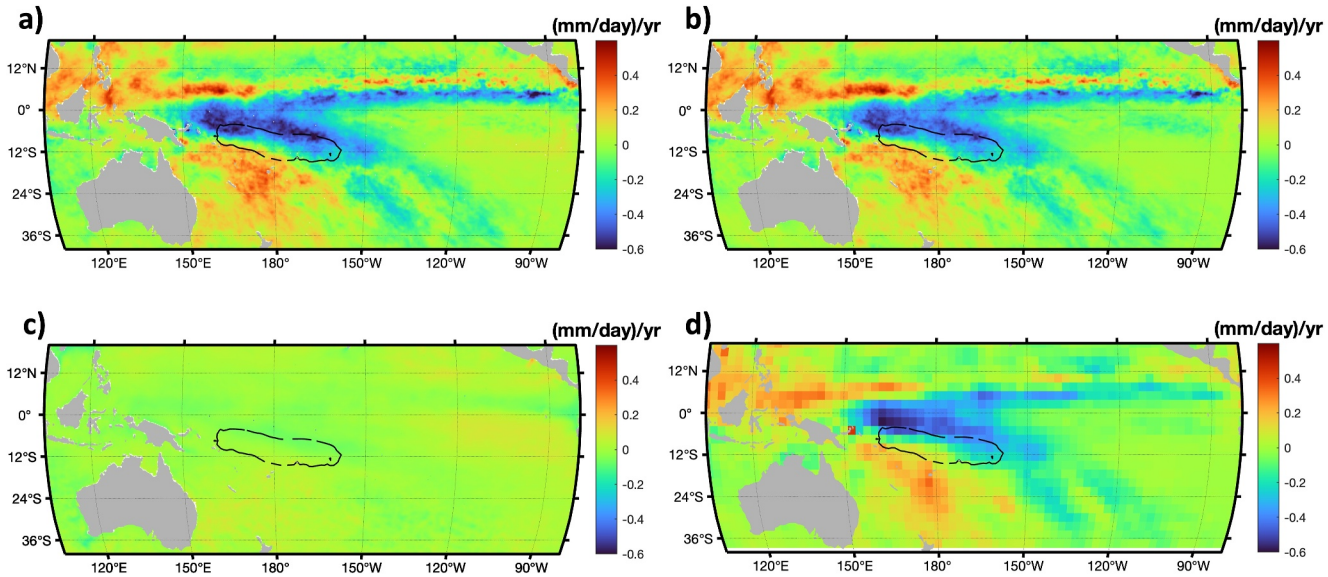

Figure 4. Trend maps over 2014–2023 based on ERA5 atmospheric reanalysis for (a) Precipitation minus Evaporation, (b) Precipitation, (c) Evaporation, and (d) Precipitation based on Global Precipitation Climatology Project product data.

Figure 4a shows the P − E trend map estimated over 2014–2023 based on ERA5 atmospheric reanalysis. Negative trends in local freshwater flux are identified just north of the area of negative halosteric sea level trends. This large scale pattern means that the local freshwater flux has decreased over 2014–2023. Figures 4b and 4c show the decadal trend maps for the precipitation and evaporation, respectively. We find no change for the evaporation field (Figure 4c) while precipitation has decreased during the considered time period. Figure 4d confirms the precipitation trend decrease over the southwestern equatorial Pacific ocean observed by GPCP data. Therefore, our results highlight a decrease in local precipitation flux over 2014–2023 consistent with an increase of salinity in the TSWPO. The identified precipitation deficit is consistent with the increased salinity of the upper ocean, which is mainly associated with the spice component (see Figure 3d).

Salinity anomalies can enter into the TSWPO to 300 m depth either by the vertical velocity time mean and/or its anomalies induced by local Ekman pumping. The time-mean Ekman pumping velocity (computed over 2014–2023, Figure 5a) shows positive values (upward velocity of ∼0.2 m/day) in the TSWPO. Figure 5b presents the map of Ekman velocity trends computed over 2014–2023. In the TSWPO, we find that the Ekman velocity trends are negative with values larger than −3 cm/day/yr indicating a decrease in upward Ekman pumping. Therefore, we do not find any local downward Ekman pumping that could advect salinity anomalies from the surface to 300 m depth in the TSWPO. Figure 5c shows the Hovmöller diagram for the spatially averaged halosteric sea level anomalies (computed over 4.5°S–15.5°S) from 2005 to 2023. We find a westward propagation of halosteric sea level anomalies from 130°W to 170°E, one positive in 2012 and one negative in 2020. This suggests a remote contribution from wind-driven dynamical changes in addition to the precipitation deficit previously presented.

4. Conclusions and Discussion

In this study, we have investigated the temperature and salinity contributions to regional sea level trends over 2014–2023. Satellite altimetry data reveal large variability in sea level trends over this period, diverging from those computed since 1993 (Cazenave & Moreira, 2022) or over 2005–2015 (Llovel et al., 2018). The non-stationarity of these regional patterns highlights the imprint of natural modes of variability on regional sea level trends inferred from satellite altimetry over the past decades. We confirm that the altimetry-based spatial trend patterns are primarily explained by steric sea level changes (inferred from Argo data). Overall, salinity has a secondary effect compared to temperature but in the TSWPO where salinity contribution tends to compensate temperature change to regional sea level trends.

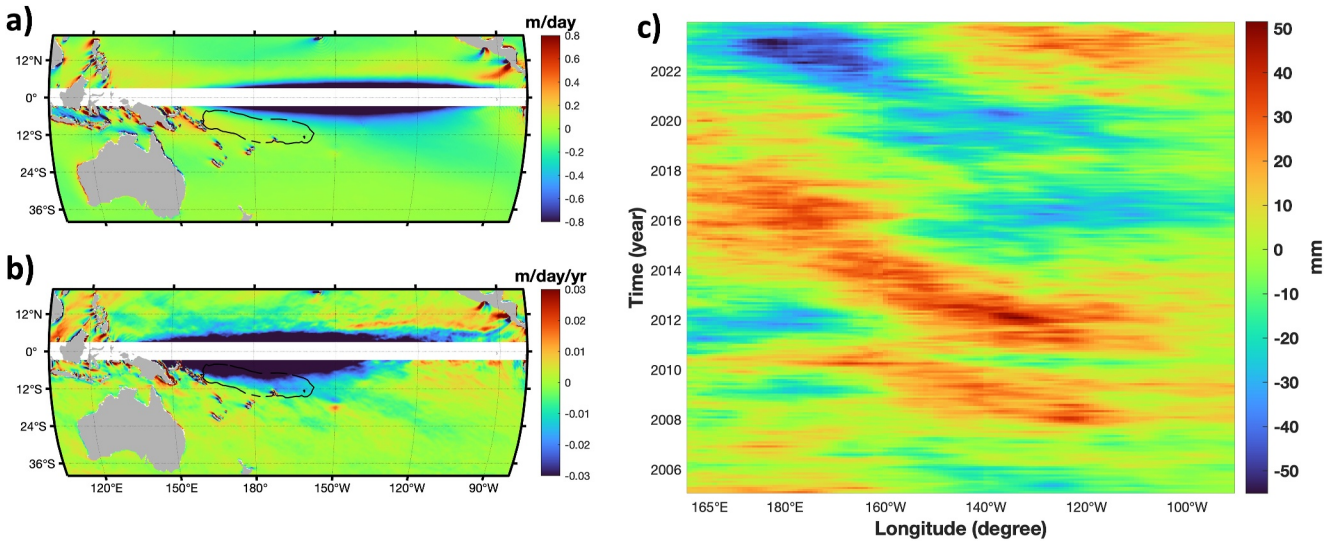

Figure 5. Maps of Ekman pumping inferred from ERA5 output: (a) time mean values, (b) trend estimates computed over 2014–2023. (c) Hovmöller plot of the halosteric sea level anomalies over 2005–2023 (over 4.5°S–15.5°S).

In the TSWPO, we find a regional sea level trend of 8.71 ± 2.31 mm/yr that is explained at 50% by the upper ocean steric sea level trend of 4.12 ± 2.33 mm/yr. Thus, we cannot neglect any contribution from the regional mass contribution (manometric sea level, Gregory et al., 2019) and/or the deep ocean contribution (Lele & Purkey, 2024). We find a compensation between the thermosteric and halosteric sea level trend highlighting the non-negligible contribution of salinity to regional sea level trends. In terms of interannual variability, we find that the thermosteric sea level explains almost all the interannual variability observed by satellite altimetry. Indeed, the Pacific equatorial interannual variability has been attributed to the El Niño Southern Oscillation imprint (Roemmich & Gilson, 2011). This is consistent with the presented results (Figure 2), as we find a sea level drop around the 2015–2016 El Niño event. During El Niño events, the warm pool, which is generally located in the western tropical Pacific, shifts eastward. This leads to a longitudinal gradient in both ocean heat content and sea level.

The present study highlights a salinity increase for the upper 400 m in the TSWPO that results from salinity advection on isopycnal surfaces and the vertical movements of the isopycnals induced by wind forcing. We find a precipitation deficit north of the TSWPO consistent with the increase of upper ocean salinity recorded by Argo data due to the spice salinity component. The evaporation does not play any significant contribution based on ERA5 data. This local precipitation decrease is confirmed by the GPCP data. Moreover, we find local contribution from upward (positive) Ekman pumping that is inconsistent with downward advection of sea surface salinity into 400 m depth. However, the observed decrease in upward Ekman pumping we find based on ERA5 data may favor an increase in salinity around 300 m by reducing upward salinity advection. Therefore, a salinity budget would help the interpretation of local wind forcing.

However, we find wave propagating signal when averaging the halosteric sea level anomalies over 4.5°S–15.5°S between 2005 and 2023. The negative halosteric sea level trends we found in the STWPO over 2014–2023 results from the positive halosteric anomaly in 2016 followed by a substantial decrease throughout 2023. Both anomalies have been created remotely near 135°W, with the negative anomaly undergoing amplification during its westward propagation. This amplification may be due to the contribution of local Ekman pumping during its propagation. Based on the Hovmöller diagram, we computed a wave speed of about 4.4 cm/s which is consistent with the theoretical value of a Rossby wave velocity of 3 cm/s at 7° of latitude. Thus, this westward wave signal may generate vertical movements of the pycnoclines in the TSWPO (Germineaud et al., 2023; Qiu & Chen, 2006). Baroclinic Rossby waves have been identified as the ocean response to wind forcing using a 1.5-layer reduced-gravity model (Qiu & Chen, 2006). This would result in a remote effect of wind-driven dynamical response to the identified salinity anomaly changes in the TSWPO that leaves imprint on regional sea level trends observed by satellite altimetry. Our results should be complemented by more quantitative investigations, such as, for instance,

numerical model simulations or a 1.5-layer reduced gravity model to confirm the processes driving this halosteric sea level decrease. However, our results emphasize the importance of salinity variability in explaining decadal sea-level trends in the TSWPO.

Data Availability Statement

Satellite altimetry data can be downloaded at DUACS (2024). Argo-based data are available at Argo (2000). ERA5 data are available at Hersbach et al. (2023). GPCP data are available at Schneider et al. (2015).

Acknowledgments
This work is a contribution to the GREAT project which is supported by the Centre National d'Etudes Spatiales (CNES) through the Ocean Surface Topography Science Team (OSTST) and to the ESA Sea Level Budget Closure project from the Climate Change Initiative Phase 2 (4000140620/23/-IBN). The authors are grateful to Sophie Cravatte and Damien Desbruyères for constructive discussions. WL and AH are both supported by CNRS. Argo data were collected and made freely available by the International Argo Program and the national programs that contribute to it (http://www.argo.ucsd.edu, http://argo.jcommops.org). The Argo Program is part of the Global Ocean Observing System. Global Precipitation Climatology Project (GPCP) Monthly Analysis Product data provided by the NOAA PSL, Boulder, Colorado, USA, from their website at https://psl.noaa.gov. The authors would like to thank two anonymous reviewers for the evaluation of the manuscript.

References

Ablain, M., Meyssignac, B., Zawadzki, L., Jugier, R., Ribes, A., Spada, G., et al. (2019). Uncertainty in satellite estimates of global mean sea-level changes, trend and acceleration. *Earth System Science Data*, *11*(3), 1189–1202. https://doi.org/10.5194/essd-11-1189-2019

Argo. (2000). Argo float data and metadata from global data assembly centre (Argo GDAC) [Dataset]. *SEANOE*. https://doi.org/10.17882/42182

Barnoud, A., Pfeffer, J., Guérou, A., Frery, M., Siméon, M., Cazenave, A., et al. (2021). Contributions of altimetry and Argo to non-closure of the global mean sea level budget since 2016. *Geophysical Research Letters*, *48*(14), e2021GL092824. https://doi.org/10.1029/2021GL092824

Bindoff, N. L., & Mcdougall, T. J. (1994). Diagnosing climate change and ocean ventilation using hydrographic data. *Journal of Physical Oceanography*, *24*(6), 1137–1152. https://doi.org/10.1175/15200485(1994)024<1137:DCCAOV>2.0.CO;2

Cazenave, A., Hamlington, B., Horwath, M., Barletta, V. R., Benveniste, J., Chambers, D., et al. (2019). Observational requirements for long-term monitoring of the global mean sea level and its components over the altimetry era. *Frontiers in Marine Science*, *6*, 582. https://doi.org/10.3389/fmars.2019.00582

Cazenave, A., & Moreira, L. (2022). Contemporary sea level changes from global to local scales: A review. *Proceedings of the Royal Society A*, *478*(2261), 20220049. https://doi.org/10.1098/rspa.2022.0049

Desbruyères, D. G., Bravo, E. P., Thierry, V., Mercier, H., Lherminier, P., Cabanes, C., et al. (2022). Warming-to-cooling reversal of overflow-derived water masses in the Irminger Sea during 2002–2021. *Geophysical Research Letters*, *49*, e2022GL098057. https://doi.org/10.1029/2022GL098057

DUACS. (2024). Global Ocean gridded L 4 sea surface heights and derived variables reprocessed 1993 ongoing [Dataset]. https://doi.org/10.48670/moi-00148

Durack, P. J., Wijffels, S. E., & Gleckler, P. J. (2014). Long-term sea-level change revisited: The role of salinity. *Environmental Research Letters*, *9*(11), 114017. https://doi.org/10.1088/1748-9326/9/11/114017

Germineaud, C., Volkov, D. L., Cravatte, S., & Llovel, W. (2023). Forcing mechanisms of the interannual ssea level variability in the midlatitude South Pacific during 2004–2020. *Remote Sensing*, *15*(2), 352. https://doi.org/10.3390/rs15020352

Gregory, J. M., Griffies, S. M., Hughes, C. W., Lowe, J. A., Church, J. A., Fukimori, I., et al. (2019). Concepts and terminology for sea level: Mean, variability and change, both local and global. *Surveys in Geophysics*, *40*, 1251–1289. https://doi.org/10.1007/s10712-019-09525-z

Häkkinen, S., Rhines, P. B., & Worthen, D. L. (2015). Heat content variability in the North Atlantic Ocean in ocean reanalyses. *Geophysical Research Letters*, *42*(8), 2901–2909. https://doi.org/10.1002/2015GL063299

Häkkinen, S., Rhines, P. B., & Worthen, D. L. (2016). Warming of the global ocean: Spatial structure and water-mass trends. *Journal of Climate*, *29*(13), 4949–4963. https://doi.org/10.1175/jcli-d-15-0607.1

Hersbach, H., Bell, B., Berrisford, P., Biavati, G., Horányi, A., Muñoz Sabater, J., et al. (2023). ERA5 hourly data on pressure levels from 1940 to present [Dataset]. *Copernicus Climate Change Service (C3S) Climate Data Store (CDS)*. https://doi.org/10.24381/cds.bd0915c6

Hersbach, H., Bell, B., Berrisford, P., Hirahara, S., Horányi, A., Muñoz-Sabater, J., et al. (2020). The ERA5 global reanalysis. *The Quarterly Journal of the Royal Meteorological Society*, *146*(730), 1999–2049. https://doi.org/10.1002/qj.3803

Hochet, A., Llovel, W., Huck, T., & Sévellec, F. (2024). Advection surface-flux balance controls the seasonal steric sea level amplitude. *Scientific Reports*, *14*(1), 10644. https://doi.org/10.1038/s41598-024-61447-y

Hochet, A., Llovel, W., Sévellec, F., & Huck, T. (2023). Sources and sinks of interannual steric sea level variability. *Journal of Geophysical Research: Oceans*, *128*(4), e2022JC019335. https://doi.org/10.1029/2022JC019335

Huang, L., Zhuang, W., Lu, W., Zhang, Y., Edwing, D., & Yan, X.-H. (2024). Rapid sea level rise in the tropical Southwest Indian Ocean in the recent two decades. *Geophysical Research Letters*, *51*(1), e2023GL106011. https://doi.org/10.1029/2023GL106011

Huffman, G. J., Adler, R. F., Bolvin, D. T., & Gu, G. (2009). Improving the global precipitation record: GPCP version 2.1. *Geophysical Research Letters*, *36*(17), L17808. https://doi.org/10.1029/2009GL040000

International Altimetry Team. (2021). Altimetry for the future: Building on 25 Years of progress. *Advances in Space Research*. https://doi.org/10.1016/j.asr.2021.01.022

Johnson, G. C., Cadot, C., Lyman, J. M., McTaggart, K. E., & Steffen, E. L. (2020). Antarctic bottom water warming in the Brazil basin: 1990s through 2020, from WOCE to deep Argo. *Geophysical Research Letters*, *47*(18), e2020GL089191. https://doi.org/10.1029/2020GL089191

Lele, R., & Purkey, S. G. (2024). Understanding full-depth steric sea level change in the Southwest Pacific Basin using Deep Argo. *Geophysical Research Letters*, *51*(12), e2023GL107844. https://doi.org/10.1029/2023GL107844

Liu, C., Liang, X., Ponte, R. M., & Chambers, D. P. (2024). "Salty Drifts" of Argo floats affects the gridded ocean salinity products. *Journal of Geophysical Research: Oceans*, *129*(9), c2023JC020871. https://doi.org/10.1029/2023jc020871

Llovel, W., Balem, K., Tajouri, S., & Hochet, A. (2023). Cause of substantial global mean sea level rise over 2014–2016. *Geophysical Research Letters*, *50*(19), e2023GL104709. https://doi.org/10.1029/2023GL104709

Llovel, W., Fukumori, I., & Meyssignac, B. (2013). Depth-dependent temperature change contributions to global mean thermosteric sea level rise from 1960 to 2010. *Global and Planetary Change*, *101*, 113–118. https://doi.org/10.1016/j.gloplacha.2012.12.011

Llovel, W., & Lee, T. (2015). Importance and origin of halosteric contribution to sea level change in the southeast Indian Ocean during 2005–2013. *Geophysical Research Letters*, *42*(4), 1148–1157. https://doi.org/10.1002/2014GL062611

Llovel, W., Penduff, T., Meyssignac, B., Molines, J.-M., Terray, L., Bessières, L., & Barnier, B. (2018). Contributions of atmospheric forcing and chaotic ocean variability to regional sea level trends over 1993–2015. *Geophysical Research Letters*, *45*(24), 13405–13413. https://doi.org/10.1029/2018GL080838

Llovel, W., Purkey, S., Meyssignac, B., Blazquez, A., Kolodziejczyk, N., & Bamber, J. (2019). Global ocean freshening, ocean mass increase and global mean sea level rise over 2005–2015. *Scientific Reports*, *9*(1), 17717. https://doi.org/10.1038/s41598-019-54239-2

Llovel, W., Willis, J., Landerer, F., & Fukumori, I. (2014). Deep-ocean contribution to sea level and energy budget not detectable over the past decade. *Nature Climate Change*, *4*(11), 1031–1035. https://doi.org/10.1038/nclimate2387

McDougall, T. J., & Barker, P. M. (2011). Getting started with TEOS----10 and the Gibbs Seawater (GSW) oceanographic toolbox. SCOR/IAPSO WG127, ISBN 978----0----646----55621----5 (p. 28).

Munk, W. (2003). Ocean freshening, sea level rising. *Science*, *300*(5628), 2041–2043. https://doi.org/10.1126/science.1085534

Nicholls, R. J., & Cazenave, A. (2010). Sea-level rise and its impacts on coastal zones. *Science*, *328*(5985), 1517–1520. https://doi.org/10.1126/science.1185782

Nicholls, R. J., Lincke, D., Hinkel, J., Brown, S., Vafeidis, A. T., Meyssignac, B., et al. (2021). A global analysis of subsidence, relative sea-level change and coastal flood exposure. *Nature Climate Change*, *11*(4), 338–342. https://doi.org/10.1038/s41558-021-00993-z

Ponte, R. M., Sun, Q., Liu, C., & Liang, X. (2021). How salty is the global ocean: Weighting it all or tasting it a sip at a time. *Geophysical Research Letters*, *48*(11), e2021GL092935. https://doi.org/10.1029/2021gl092935

Qiu, B., & Chen, S. (2006). Decadal variability in the large-scale sea surface height field of the South Pacific Ocean: Observations and causes. *Journal of Physical Oceanography*, *36*(9), 1751–1762. https://doi.org/10.1175/JPO2943.1

Roemmich, D., Alford, M. H., Claustre, H., Johnson, K., King, B., Moum, J., et al. (2019). On the future of Argo: A global, full-depth, multi-disciplinary array. *Frontiers in Marine Science*, *6*, 439. https://doi.org/10.3389/fmars.2019.00439

Roemmich, D., & Gilson, J. (2009). The 2004-2008 mean and annual cycle of temperature, salinity and steric height in the global ocean from the Argo program. *Progress in Oceanography*, *82*(2), 81–100. https://doi.org/10.1016/j.pocean.2009.03.004

Roemmich, D., & Gilson, J. (2011). The global ocean imprint of ENSO. *Geophysical Research Letters*, *38*(13), L13606. https://doi.org/10.1029/2011GL047992

Schneider, U., Becker, A., Finger, P., Meyer-Christoffer, A., Rudolf, B., & Ziese, M. (2015). GPCC monitoring product: Near real-time monthly land-surface precipitation from rain-gauges based on SYNOP and CLIMAT data [Dataset]. https://doi.org/10.5676/DWD_GPCC/MP_M_V5_100

Stammer, D., Cazenave, A., Ponte, R. M., & Tamisiea, M. E. (2013). Causes for contemporary regional sea level changes. *Annual Review of Marine Science*, *567*(1), 21–46. https://doi.org/10.1146/annurev-marine-121211-172406

Tajouri, S., Llovel, W., Sévellec, F., Molines, J.-M., Mathiot, P., Penduff, T., & Leroux, S. (2024). Simulated impact of time-varying river runoff and Greenland freshwater discharge on sea level variability in the Beaufort Gyre over 2005–2018. *Journal of Geophysical Research: Oceans*, *129*(9), e2024JC021237. https://doi.org/10.1029/2024JC021237

Volkov, D. L., Lee, S. K., Landerer, F. W., & Lumpkin, R. (2017). Decade-long deep-ocean warming detected in the subtropical South Pacific. *Geophysical Research Letters*, *44*(2), 927–936. https://doi.org/10.1002/2016gl071661

Wong, A. P. S., Wijffels, S. E., Riser, S. C., Pouliquen, S., Hosoda, S., Roemmich, D., et al. (2020). Argo data 1999-2019: Two million temperature-salinity profiles and subsurface velocity observations from a global array of profiling floats. *Frontiers in Marine Science*, *7*, 700. https://doi.org/10.3389/fmars.2020.00700

Zilberman, N. V., Thierry, V., King, B., Alford, M., Andre´, X., Balem, K., et al. (2023). Observing the full ocean volume using deep Argo floats. *Frontiers in Marine Science*, *10*, 1287867. https://doi.org/10.3389/fmars.2023.1287867